Eurasian Journal of Physics and Functional Materials

2020, 4(1), 13-18

Manifestations of pear-shaped clusters in collinear cluster tri-partition of ^{252}Cf

Yu.V. Pyatkov*,[1,2], D.V. Kamanin[2], A.A. Alexandrov[2], I.A. Alexandrova[2], Z.I. Goryainova[2], E.A. Kuznetsova[2], A.O. Strekalovsky[2], O.V. Strekalovsky[2], V.E. Zhuchko[2], V. Malaza[3]

[1]National Nuclear Research University MEPhI (Moscow Engineering Physics Institute), Moscow, Russia

[2]Joint Institute for Nuclear Research, Dubna, Russia

[3]University of Stellenbosch, Faculty of Military Science, Military Academy, Saldanha, South Africa

E-mail: yvp_nov@mail.ru

DOI: **10.29317/ejpfm.2020040102**
Received: 10.01.2020 - after revision

Specific mode of the collinear cluster tri-partition of the ^{252}Cf nucleus is discussed. The structure manifests itself as a rhombic-spiral structure in the fission fragments correlation mass distribution.

Keywords: ternary fission, shell corrections, nuclear clusters.

Introduction

Most of our experiments in recent years were dedicated to the study of new multibody at least ternary decay channel of low excited heavy nuclei [1, 2]. Due to specific features of the effect, it was called by us collinear cluster tri-partition (CCT). Now we have an entire collection of different CCT manifestations, observed through the linear structures in the mass correlation distributions of the decay products. Some of the structures look like the straight lines satisfying the condition

($M_1 + M_2$) = const, where M_1 and M_2 are the fission fragments (FFs) detected in coincidence while their total mass is less than the mass of the fissioning nucleus. The mass of the missed fragment is obviously constant for the fission events forming each such line. As far as we know, similar structures had been never discussed in the past.

Experimental and results

The experiment Ex1 was carried out at the COMETA-F spectrometer in the FLNR (JINR, Dubna, Russia). The layout of the spectrometer is shown in Figure 1.

It is double-armed time-of-flight FFs spectrometer consisting of four mosaics of PIN diodes, and two timing detectors. Signals from all the detectors were digitized in 0.2 ns increments by the fast flash-ADC (Amplitude to Digital Convertor) CAEN DT5742. For the proper reconstruction of the FF mass, if a PIN diode is used for the measurement of both FF energy and velocity one should take into account so called "pulse height defect" and "plasma delay" [3, 4]. This is exactly what is done in the data processing approach proposed by us in [5, 6]. In the latter publication new "parabola time-pickoff" method used in Ex1 is described.

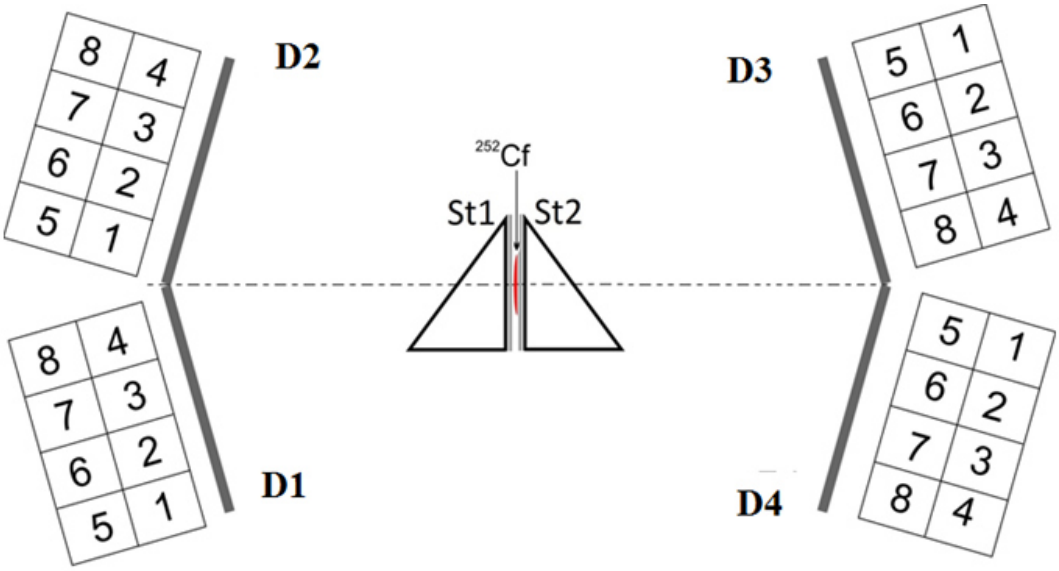

Figure 1. Layout of the COMETA-F setup. A spectrometric source of ^{252} Cf (sf) is located in between two microchannel plates based timing detectors St1 and St2 giving "start" signals. Four mosaics (D1-D4) of eight PIN diodes each provide the signals for measurement of both the FF time-of-flight and energy. The FF mean flight pass does not exceed fifteen centimeters.

FFs mass correlation distributions in the region of the "Ni-bump" obtained in Ex1 and Ex2 [1] are presented in Figure 2. Due to the background conditions of the experiment Ex1, the events with the energy of the light fragment in the range $E_2 = (6 \div 30)$ MeV were selected (Figure 2a).

The data from Ex1 along with the presence of the lines at the mass numbers M_2 = (128, 68, 72) unmarked in the Figures 1, 2, 3 correspondingly, show some additional structures. A rhombic-spiral structure in the lower right corner of Figure 2a that resembles a rose depiction we called "nuclear rose". It consists of the family of lines $M_1 + M_2$ = const and several lines almost perpendicular to them.

The lines of the first sort (marked by the numbers 1-6 in Figure 3a) will be analyzed in the next section while a discussion of the latter is below the scope of this paper.

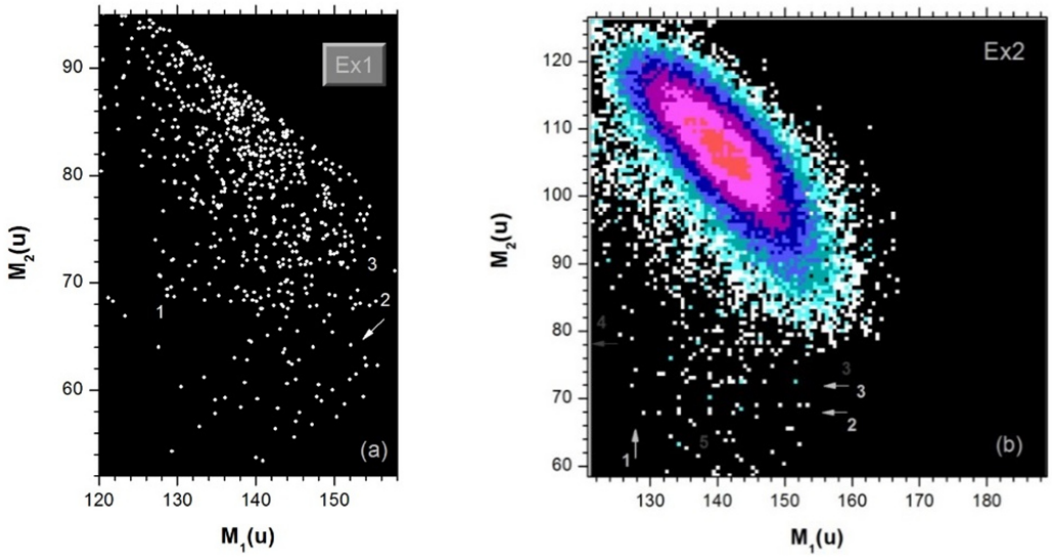

Figure 2. FFs mass correlation distributions from ^{252}Cf(sf) obtained in Ex1-(a). Specific rhombic-spiral structure in the bottom of the figure ("nuclear rose") is marked by an arrow. The distribution is compared with that obtained earlier in Ex2 [1]-(b).

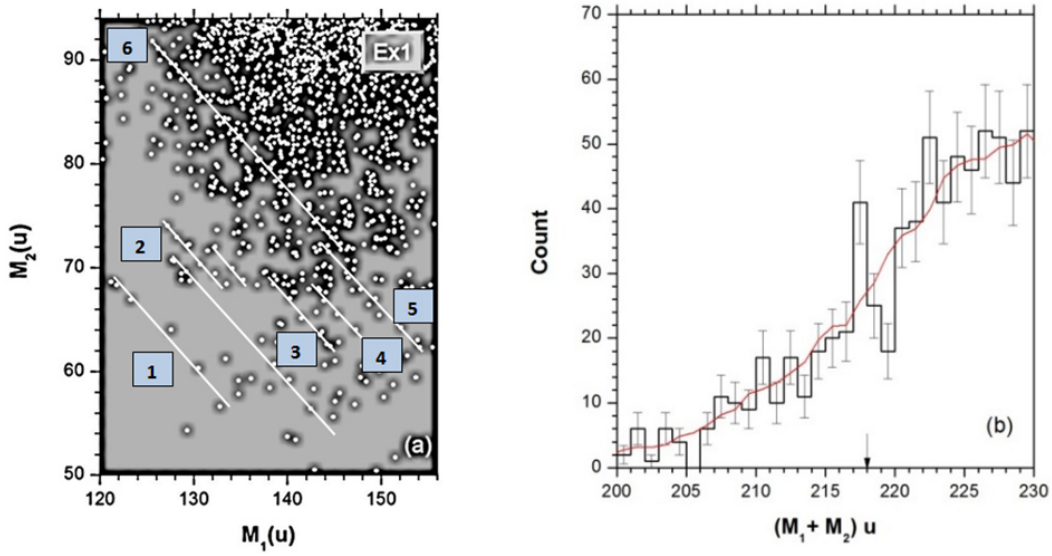

Figure 3. Mass-correlation distribution from Ex1-(a). The tilted numbered lines in white meet the condition $M_1 + M_2 =$ const. Projection of the distribution along such direction in the vicinity of line 6-(b). The peak centered at 218u marked by the arrow exceeds by more than two sigma the level obtained by smoothing the original spectrum.

Two structures from Figure 3a are presented in Figure 4 in the larger scale. Expected prescission cluster composition of the decaying system for the events marked by arrows are shown in insets. Each list of the clusters begins with the "missed" nucleus. Its mass corresponds to the missing mass in the expression $M_1 + M_2 =$ const.

Different projections of the mass correlation distribution from Ex1 are shown in Figure 5. As can be inferred from the Figure 5a, the statistics in Ex1 is approximately three times more than that in Ex2. A total yield of two Ni peaks in Ex1 does not exceed 10^{-4} per binary fission which agrees with our previously obtained

value. The data of Ex2 indicated that the heavy clusters in the ternary prescission configurations are predominantly magic nuclei (Table 1 in [7]). Noticeably large statistics in Ex1 allowed us to confirm previous observation. The projection of the distribution shown in Figure 5b onto M_1 axis for the range of M_2 = (65-76)u clearly demonstrates increased yield of the heavy fragments corresponding to the magic isotopes of ^{128}Sn, ^{134}Te, ^{140}Xe, ^{144}Ba, ^{150}Ce, ^{154}Nd (their masses are marked in Figure 5b by arrows).

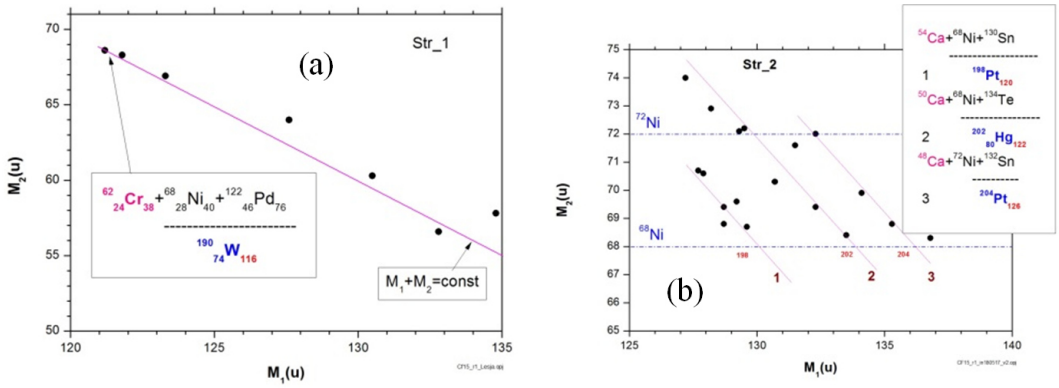

Figure 4. Two structures from the Figure 3a in the larger scale. Cluster compositions for the events marked by arrows are shown in insets.

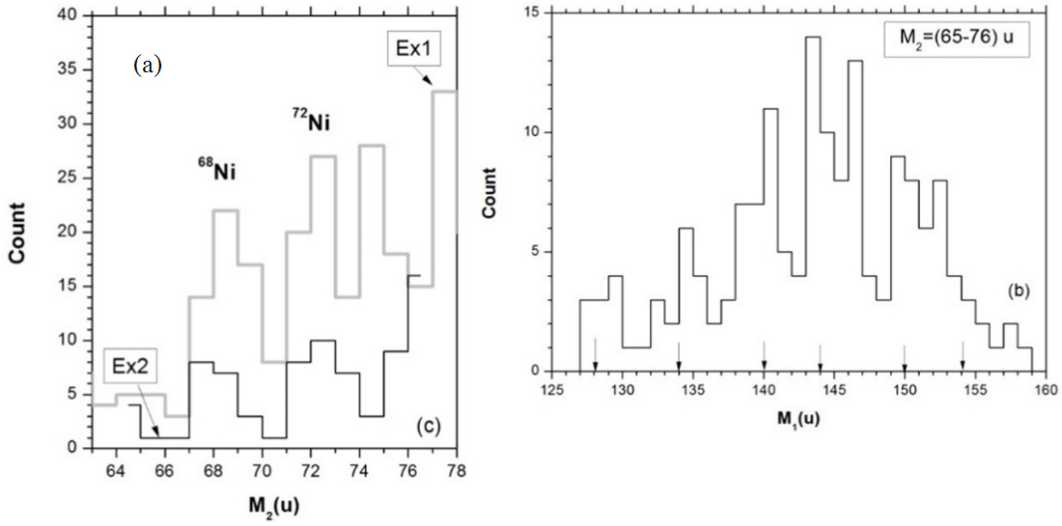

Figure 5. Projections of the mass-correlation distributions obtained in Ex1 and Ex2 onto M_2 axis-(a). Projection of the mass-correlation distribution from Ex1 onto M_1 axis under condition M_2 = (65-76)u-(b).

Discussion

For the first time we had observed linear structures meeting the condition $M_1 + M_2$ = const in our experiment (Ex3) at the FOBOS setup based on the gas-filled detectors [8]. The linear ridges corresponding to the constant missing masses were revealed as a fine structure in the mass correlation plot collected with good statistics. Later, using COMETA spectrometer based on the mosaics of PIN diodes, we also observed the structures under discussion (Ex2), but the data suffered from

small statistics [1]. Parameters of all linear structures observed so far in the region of so called "Ni-bump" are presented in Table 1.

Table 1.
Parameters of the linear structures shown in Figure 3a.

Parameters of the structures observed				
Str No.	Missing fragment	Heavy magic core	Number of neutrons	Experiments
1	^{62}Cr	^{190}W	116	Ex1
2	^{48,50,54}Ca	^{198}Pt, ^{202}Hg, ^{204}Pt	120, 122, 124	Ex1& Ex2
3	^{44}S	^{208}Pb	126	
4	^{40}Si	^{212}Po	128	Ex1& Ex3
5	^{36}S	^{216}Po	132	
6	^{34}Si(N=20)	^{218}Po	134	Ex1

As can be inferred from Figure 6, showing the shell corrections map [9], the numbers of neutrons in the heavy magic cores (the forth column in Table 1) manifest themselves through the discussed structures correspond to the valley of negative shell corrections. In the recent publication [10] on the study of pear-shaped nuclei, it was noted that octupole correlations enhanced at the magic neutron numbers 34, 56, 88, 134. Thus, it is reasonable to expect that the nuclei having 116-134 neutrons would be pear-shaped and show magic properties. According to the calculations, for instance [11], fissioning system becomes pear-shaped at the beginning of the descent from the fission barrier, at least in the most populated fission valley of the potential energy surface.

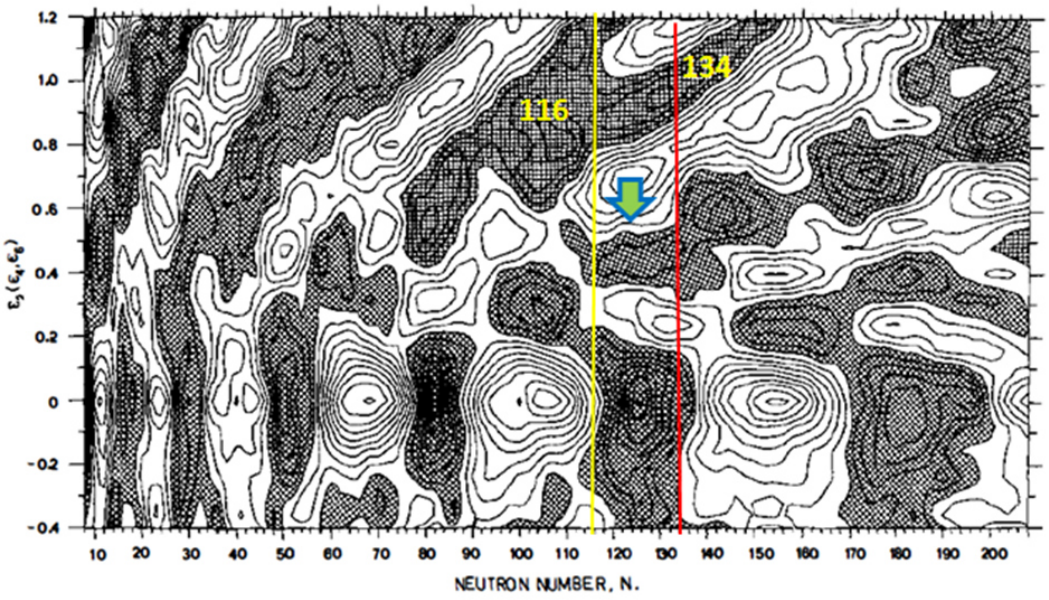

Figure 6. Shell energy diagram [10] depending on neutron number and deformation. Areas corresponding to negative shell energy are shaded, and the contour separation is 1 MeV.

We propose the following scenario of the process leading to the formation of the structures under discussion. At the initial stage of the descent from the fission barrier, the fissioning nucleus undergoes transformation from a prolate to more

complicated shape. The nucleus of such shape consists of a heavy magic octupole deformed core and the light cluster in contact with the thin edge of the "pear". At further elongation the core takes dumbbell-like shape with longer and longer neck between the heavy and light parts of the dumbbell. The mass of the light cluster stays unchanged. After the first rupture in the neck, a heavy fragment and a di-nuclear system consisting of the light cluster and some part of the neck fly apart. Later, due to the second rupture, the light cluster and the light FF become free. In general, the kinematics of the process seems to be similar to that discussed in [7].

Conclusion

Based on the new data we clarify a mechanism of the CCT mode similar to heavy ion radioactivity [8]: octupole deformed magic core plays the same role as magic Pb cluster in the "Lead radioactivity".

Acknowledgments

This work was supported by the research project No. 18-32-0053 of the Russian Foundation for Basic Research (RFBR), and by the MEPhI Academic Excellence Project (Contract No. 02.a03.21.0005, 27.08.2013) of the Russian Science Foundation.

References

[1] Yu.V. Pyatkov et al., Eur. Phys. J. A **48** (2012) 94-110.
[2] D.V. Kamanin, Yu.V. Pyatkov, Clusters in Nuclei Volume 3, Lecture Notes in Physics (Springer, 2013) **875** 69 p.
[3] S.I. Mulgin et al., Nucl. Instrum. Meth. **388** (1997) 254.
[4] H.O. Neidel, H. Henschel, Nucl. Instr. and Meth. **178** (1980) 137.
[5] D.V. Kamanin et al., Conference proceedings of the Int. Symp. on Exotic Nuclei "EXON-2014", Kalaningrad (2015) 677.
[6] D.V. Kamanin et al., Izvestiya Rossiiskoi Akademii Nauk. Seriya Fizicheskaya **82**(6) (2018) 804-807. (in Russian)
[7] Yu.V. Pyatkov et al., Phys. Rev. C **96**(6) (2017) 064606.
[8] Yu.V. Pyatkov et al., Eur. Phys. J. A **45** (2010) 29-37.
[9] S. Aberg et al., Annu. Rev. Nucl. Part. Sci. **40** (1990) 439-527.
[10] L.P. Gaffne et al., Nature. V. **497** (2013).
[11] Yu.V. Pyatkov et al., Nucl. Phys. A **624** (1997) 140.